

Development of a ToF setup with an ion-guide for characterization of electrospray microthrusters

IEPC-2013-413

Presented at the 33rd International Electric Propulsion Conference,
The George Washington University • Washington, D.C. • USA
October 6 – 10, 2013

Subha Chakraborty¹ Simon Dandavino², Caglar Ataman³, Daniel G. Courtney⁴
and Herbert Shea⁵

Ecole Polytechnique Fédérale de Lausanne (EPFL), Neuchatel, 2002, Switzerland

Abstract: Electrospray microthrusters are a very promising micro-propulsion system which can potentially provide very high specific impulse ($I_{sp} \sim 3000s$). In this paper, we report on the development of a time-of-flight (ToF) measurement setup for characterization of the spray composition of the electrospray sources. This setup consists of an electrostatic ion-guide built with 13 cascaded single-stage Einzel lenses along with a 65 cm long flight tube to focus the emitted charges on a Faraday cup detector. The distributed lens ensures a large fraction of the emitted beam can be collected, even when the beam divergence is high. Simulations of the focusing capabilities of the ion guide have been performed and are compared with a single stage Einzel lens, with excellent agreement. The efficiency of the lens has been characterized with microfabricated capillary electrospray devices and with electrochemically etched tungsten needles.

Nomenclature

I_{sp}	=	Specific impulse
ToF	=	Time of flight
q	=	Charge
m	=	Mass
$EMI-BF_4$	=	1-ethyl-3-methylimidazolium tetrafluoroborate
SOI	=	Silicon-on-insulator
V_{em}	=	Extraction voltage
V_{lens}	=	Lens voltage
L	=	Length of flight tube
D	=	Diameter of the Faraday cup
I_{det}	=	Detected current
I_{em}	=	Emitted current
θ_{det}	=	Detection half-angle
θ_{em}	=	Emission half-angle
d	=	Diameter of a lens electrode
l	=	Length of a lens electrode
DRIE	=	Deep reactive ion etching

¹ PhD student, LMTS-IMT-EPFL, Subha.chakraborty@epfl.ch.

² PhD student, LMTS-IMT-EPFL, simon.dandavino@epfl.ch.

³ Group Leader IMTEK (former post doc., LMTS), caglar.ataman@imtek.uni-freiburg.de.

⁴ Post-doc, LMTS-IMT-EPFL, daniel.courtney@epfl.ch.

⁵ Professor, LMTS-IMT-EPFL, herbert.shea@epfl.ch.

I. Introduction

TIME of flight (*ToF*) mass spectrometers are analytical instruments that distinguish charged particles based on their different velocities due to different charge (q) over mass (m) ratios. They measure the flight time of the charges from which the q/m can be evaluated. In principle, *ToF* mass spectrometers do not have a lower limit of resolution except for detectability of the measurement instrument¹. In this paper, development of a *ToF* setup for characterization of ion species emitted from electrospray sources is reported. The electrospray sources are microfabricated on silicon-on-insulator (SOI) wafers for generating thrust for nano- and pico-satellites with a very high specific impulse². We have also used electrochemically sharpened and roughened tungsten needles³, which emits pure ions by electrospray, for characterization of the lens. The devices work on the principle of emitting charged particles (ions/charged droplets) from the emitter filled/wetted with ionic liquids (e.g. *EMI-BF₄*) by applying a high extraction potential (typically $\sim 1\text{--}2$ kV) in high vacuum conditions ($\sim 10^{-6}$ Pa). Depending on the extraction potential (V_{em}), geometry of the emitter device and environmental conditions, the devices can spray pure ions (typically ~ 100 nA) or charged droplets (~ 1 μ A) of positive and negative polarity^{2,3,4,5}. While pure ion emission can potentially produce very high *Isp*, droplet emission results in low *Isp* but higher thrust.

The spray composition can be analyzed by distinguishing the ions from the droplets based on their q/m ratio by *ToF* measurement. However, it has been observed that emission takes place over an emission half-angle up to nearly⁵ 40° . It is also observed that the emitted charges may have a kinetic energy distribution among themselves⁴. In order to collect the q/m information from the emission, either a very large detector is required to be placed to collect most of the emitted charges after travelling for a measurable flight time or the charges can be focused during their flight by electrostatic lens on a small detector. Having a large detector after a long flight path requires a large vacuum chamber while focusing on a small detector can reduce the size of the vacuum chamber for spraying. Electrostatic Einzel lenses are usually made of three cylindrical electrodes⁶ with the central electrode at high voltage and the other two at ground potential to deflect charges towards the axis of the lens. For a given lens voltage, the focal length of the lens depends on the angle and kinetic energy of the charges and it is therefore difficult to focus the entire emitted beam on the small detector for a given lens voltage unless the under-focused or over-focused charges are further deflected using other lens stages.

In order to collect those dispersed charges, an electrostatic lens-system using 13 cascaded stages of single-stage Einzel lenses has been designed and tested. This lens system sits inside a 0.65 m long and 70 mm inner-diameter flight tube between the emitter and the detector. This lens system compensates for the under-focusing and over-focusing in each stage from the previous stage and thus guides the charges over a wide emission angle and energy spread on a small (~ 10 mm diameter) Faraday cup detector. Simulation shows that the ion-guide can perform focusing of all charges within nearly 23° emission half-angle with respect to the axis of the lens and for a 40° emission half-angle⁵ the Faraday-cup can detect 30-35% of the charges if the lens voltage V_{lens} is set between $0.8 \times V_{em}$ and V_{em} .

In the next section, the design and performance simulation of the ion-guide is presented. In section III, the details of the *ToF* setup are explained. In section IV, the experimental results are described.

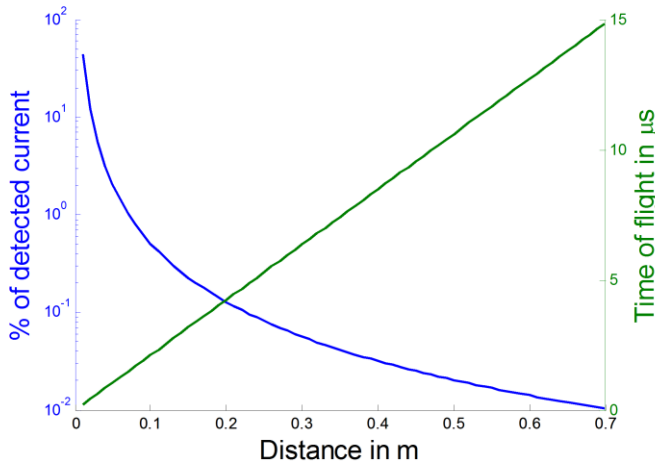


Figure 1. Calculated variation of the percentage of emitted current that can be detected and the flight time with the length of the flight tube. ($V_{em} = 1$ kV, $\theta_{em} = 40^\circ$, $D = 10$ mm)

II. Ion guide design

Since emission half-angle is nearly 40° , there is a trade-off between the current collected in a small detector and a long flight time. The flight time *ToF* is given by the expression

$$ToF = L \sqrt{\frac{m}{2qV_{em}}} \quad (1)$$

where L is the length of the flight tube. The current detected by a Faraday cup detector with a diameter D is approximately given by

$$I_{det} = I_{em} \left(\frac{\theta_{det}}{\theta_{em}} \right)^2 \quad (2)$$

where I_{em} is the emitted current, θ_{det} is the half-angle subtended by the Faraday cup at the tip of the emitter given by

$$\tan\theta_{det} = \frac{D}{2L} \quad (3)$$

θ_{em} is the emission half-angle. In the Fig. 1 the variation of the detected current and the *ToF* for the BF_4^- ions are shown as function of the length of the flight tube. It is assumed that the emission takes place uniformly with an emission half-angle $\theta_{em} = 40^\circ$, $V_{em} = 1000$ V and the Faraday cup diameter is $D = 10$ mm. The plots show that if the detector is placed away from the emitter, the flight time increases eliminating the requirement of very high bandwidth of detection circuit; but the detected current is very low, requiring very high trans-impedance gain. On the other hand, if the detector is placed close to the device, it detects significant amount of current but the flight time is very low and a very high bandwidth is required for the detection circuit to detect and separate the flight times. For example, if a detector is placed at 100 mm from the emitter, for pure ionic mode emission of 100 nA BF_4^- ions, the detector receives only 500 pA current with a flight time 2.1 μs and detection with commercially available trans-impedance amplifiers will not be possible unless the charges are focused on the detector with electrostatic lens to increase the detection current.

In the design, a flight length of 0.65 m is chosen for 14 μs flight time of the BF_4^- ion at 1000 V emission voltage. This length is chosen from a commercially available flight tube with inner diameter 70 mm so that square metallic plates with 51 mm side commercially available from KimballPhysics⁷ can fit inside the tube without additional need of aligning them to the axis of the tube. Simulation has been performed for the lens configuration with Simion ion simulator using the commercially available dimensions from KimballPhysics⁷. First, simulation has been performed for a single Einzel lens configuration with metallic plates with circular opening as grounded electrodes and cylindrical structure as the deflecting electrode as shown in Fig. 2(a). In these simulations, the ratio of the number of charges detected by the detector and the number of charges emitted is defined as Lens efficiency

$$\text{Lens efficiency} = \frac{I_{det}(V_{lens})}{I_{em}} \quad (4)$$

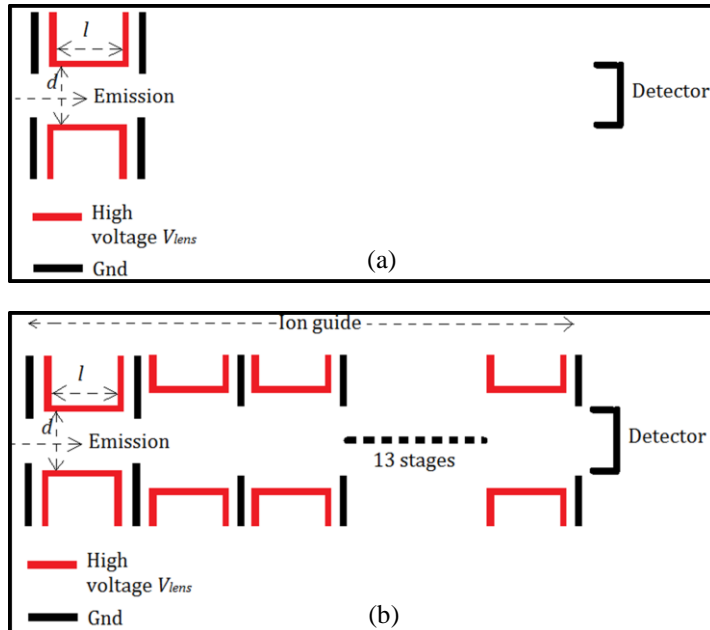


Figure 2. (a) Schematic cross-section of a single-stage lens, (b) Schematic of the ion-guide

and is plotted in Fig. 3 as a function of the ratio of V_{lens}/V_{em} . It has been observed that the cylindrical electrode with commercially available $d = 25$ mm diameter and $l = 25$ mm length can focus up to 10% of the emitted charges on the 10 mm diameter detector at the end of the *ToF* tube for $V_{lens}/V_{em} = 0.875$. It is also observed that although nearly 40% of the charges come out of the lens, nearly 75% of it is either under-focused or over-focused because of their large emission angle and they don't reach the detector as shown in Fig. 4(a).

In order to collect these dispersing charges, the single stage lens with $d = 25$ mm and $l = 25$ mm is augmented by additional lens-stages all along the length of the flight tube as shown in Fig. 2(b) to compensate for the deflection of the charges away from axis as opposed to the single stage lens as shown in Fig. 4(b). These stages comprise of grounded plate electrodes and cylindrical high-voltage deflecting electrodes at the same lens voltage as the first stage with inner diameter 37.5 mm and length 37.5 mm.

As shown in Fig. 3, this ion-guide can focus 25–35% of the total emitted charges with V_{lens}/V_{em} between 0.8 to 1.0. This suggests that for a lens voltage 800 V, the *ToF* setup can detect significant amount of charges with kinetic energy spread between 800 V and 1000 V. However, these simulations are performed with the assumption that the

emission current density is uniform over 40° half-angle. Since most of the current density is concentrated within 30° half-angle⁵, the efficiency can be higher in practice.

In Fig. 5, the variation of the maximum emission angle up to which the ion-guide can focus the charges on the detector for different V_{lens}/V_{em} is shown. This shows that the *ToF* setup can focus all the charges within a half-angle

nearly 23° as opposed to only 10° for the single-stage lens.

Although the ion-guide can focus charges over wider energy range and emission angle, it has an effect of increasing the flight time due to repeated deceleration stages all along the flight tube. This delay can be characterized by the *ToF correction factor* defined here by

$$ToF \text{ correction factor} = \frac{ToF(V_{lens}, V_{em})}{L \sqrt{\frac{m}{2qV_{em}}}} \quad (5)$$

In Fig. 6, the simulated variation of the *ToF correction factor* is plotted as function of V_{lens}/V_{em} . As seen from the plots, for $V_{lens}/V_{em} = 0.8$, where the ion-guide detects maximum number of charges, the *ToF* increases by a factor of 1.6 from its value given by equation (1).

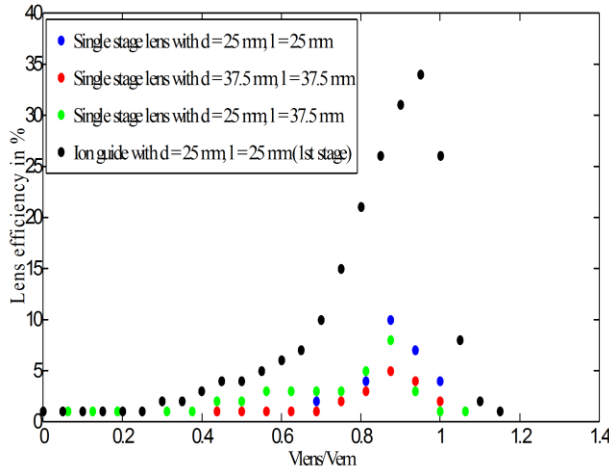


Figure 3. Simulation of variation of the lens efficiency of different Einzel lens configurations and of the ion-guide with V_{lens}/V_{em}

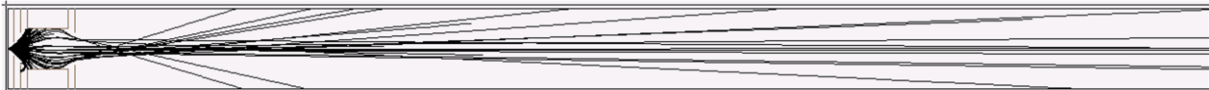


Figure 4(a). Simulated ion trajectories in the Single lens case with $V_{em} = 1000$ V and $V_{lens} = 800$ V. $d = 25$ mm, $l = 25$ mm. Emission starts at the left end of the image and ions are detected on the right end.

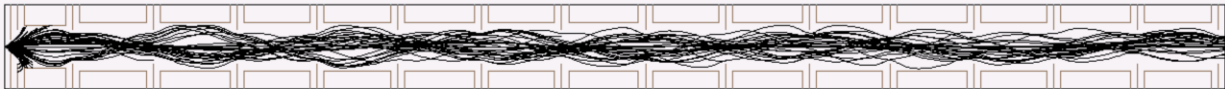


Figure 4(b). Simulated ion trajectories in the Ion-guide case with $V_{em} = 1000$ V and $V_{lens} = 800$ V. $d = 25$ mm, $l = 25$ mm for the first stage, $d = 37.5$ mm, $l = 37.5$ mm for all the other stages.

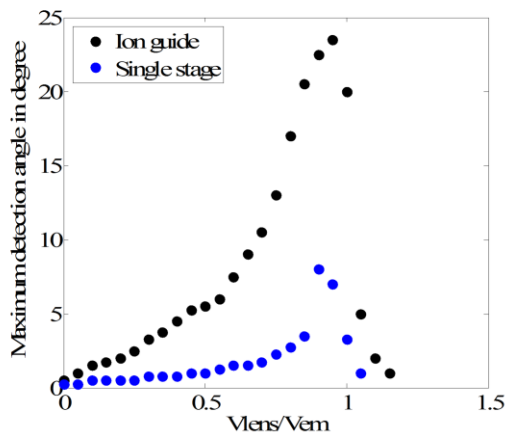


Figure 5. Simulation of variation of the max. half-angle up to which 100% charges can be detected with V_{lens}/V_{em} for a single stage lens and the ion-guide

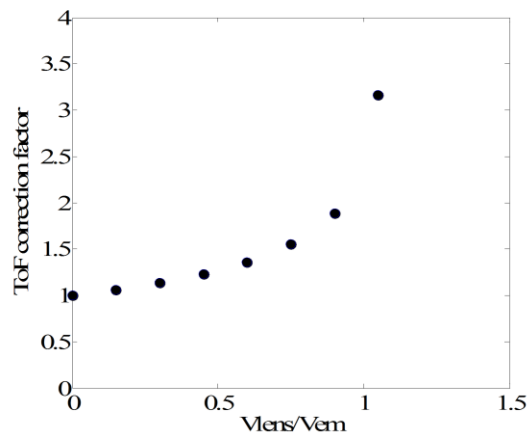


Figure 6. Simulation of variation of the ToF correction factor with V_{lens}/V_{em}

III. Experimental setup

A. ToF setup

In Fig. 7, a schematic of the experimental setup is shown. This consists of a vacuum chamber with the flight tube as shown in Fig. 8(a) and the ion-guide, as shown in Fig. 8(b) is aligned with the tube inside it between the emitter assembly and the Faraday cup detector. EMCO high voltage power supplies and high voltage relays have been used for emission voltage and lens voltages in both polarities of operation. A gate electrode with a grid of nearly 80% transparency between the emitter and the ion-guide which is switched from high voltage (typically $1.1 \times V_{em}$) to 0 V within 100 ns

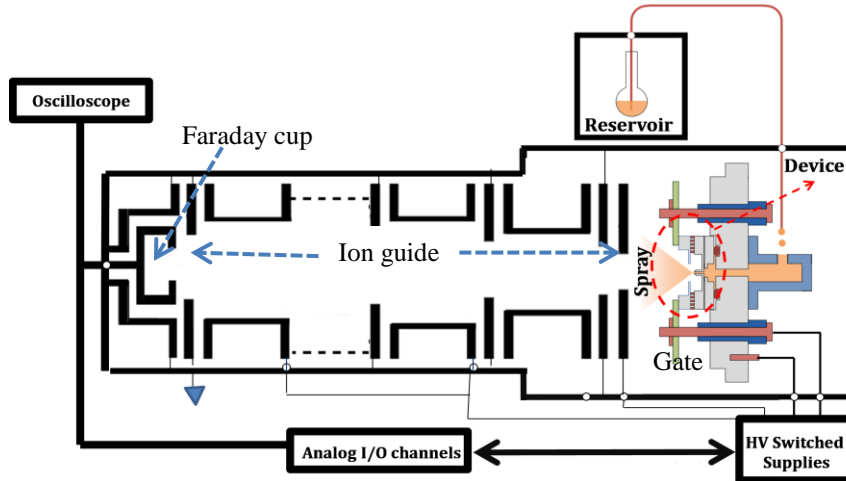


Figure 7. Schematic of the complete ToF measurement setup

for ToF measurements. A Femto DHPCA 100 high speed trans-impedance amplifier is used to convert the detected current to voltage.

B. The emitter

We characterized with two types of emitters. The capillary emitters are micro-fabricated on silicon-on-insulator (SOI) wafers. The capillary is fabricated using deep reactive ion etching (DRIE) process with 8–11 μm inner diameter and 100 μm height^{2,8}. The extractor is created on another SOI wafer with diameter varying from 150 μm to 300 μm . The two wafers are then bonded by thermal compression and individual emitter devices are diced^{2,8}. In Fig. 9, a scanning electron microscope (SEM) image of the emitter device is shown⁵. The ionic liquid EMI-BF₄ is filled in the reservoir on the backside of the emitter and the liquid then fills the emitter by capillary process without

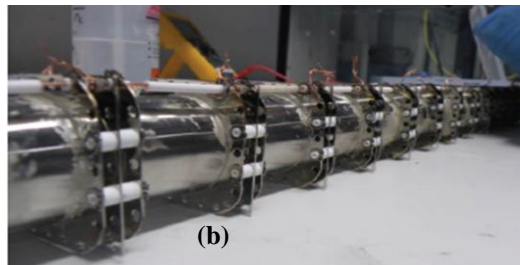
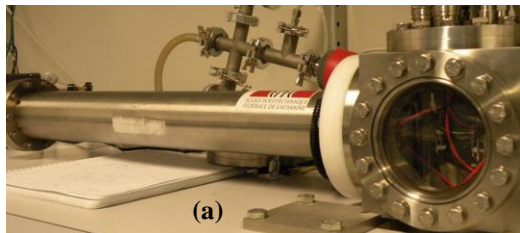


Figure 8. (a) The ToF setup with the spray assembly and the ion-guide inside, detector on the left-side end of the tube, (b) The ion-guide with cascaded deflection and ground electrodes.

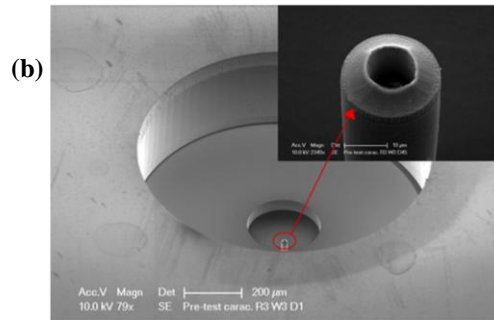
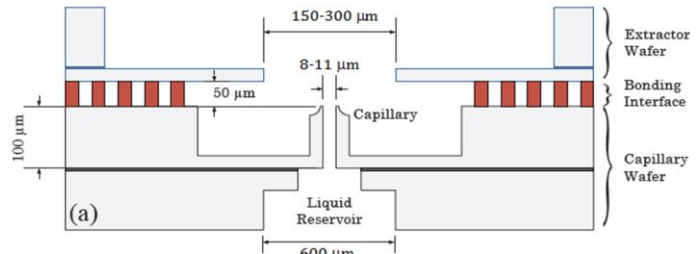


Figure 9. (a) Schematic cross-section of the complete electro-spray microthruster, (b) SEM image.

applying external pressure. Emission voltage is applied between the capillary and the extractor to extract charges from the tip of the liquid from the capillary.

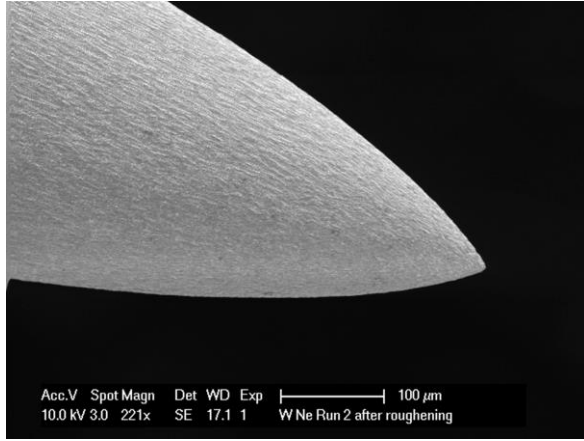


Figure 10. SEM image of electrochemically sharpened and roughened tungsten needle

To characterize the lens with pure ionic emitters, without possibility of droplet disintegration, we tested electrochemically sharpened and roughened tungsten needles fabricated in the process reported by Lozano and Martínez-Sánchez in 2005³. These needles have typically 10–15 μm radius of curvature at the tip and they are externally wetted with EMI-BF_4 to emit pure ions. These devices are previously reported to emit in pure ionic regime within 15–20° half-angle⁷. In Figure 10, SEM image of a tungsten needle is shown.

IV. Test results

A. Electrostatic Lens efficiency

In Fig. 11, the lens efficiency of the microfabricated emitters for different emission voltages in positive and

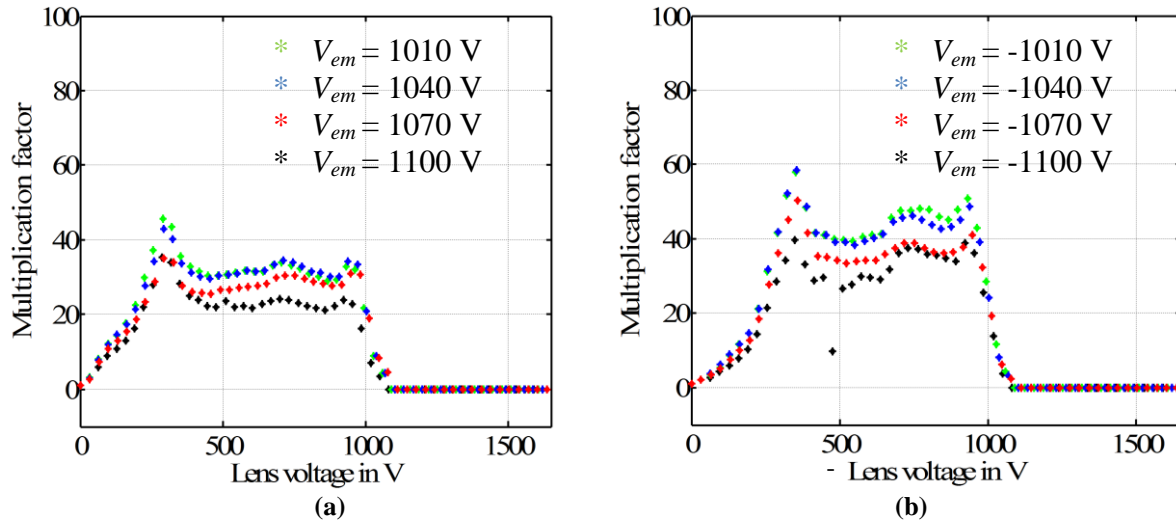


Figure 11. Measured Lens efficiency for different emission voltages in positive (a) and negative (b) polarities respectively from microfabricated electro spray device with 300 μm extractor diameter.

negative polarities are shown. The lens voltage is varied from 0 V to ± 1650 V and the emitter current and detector current are measured. The plots show that the efficiency of the lens is between 20% and 35% for the positive polarity and between 30% and 40% for negative polarity. The 30–40% efficiency, as opposed to the simulated value of 25–35%, may be due to the fact that the emission current density is mostly concentrated within 30° half-angle as mentioned before⁵. It is also observed from the plots that as the emission voltage increases, the efficiency reduces. This is because as the emission voltage increase, the emission spreads over higher half-angle⁵.

It is observed that the range of values for V_{lens} with the maximum efficiency is significantly larger than the simulation results ($0.8 \times V_{em}$ to V_{em}). Also there is a peak between 200 V and 300 V which is unclear. It is possible that the emission kinetic energy is spread over a wide range for the emitters. There can be solvated ions and large charged droplets emitted and then disintegrated into smaller droplets or ions, spreading the kinetic energy range of the emitted species over a wide range.

Lens efficiency tests are performed with the needles and in Fig. 12, the variation of the lens efficiency is shown. Due to smaller emission angle the efficiency is higher than the capillary emitters and the maximum efficiency is achieved with V_{lens}/V_{em} having a value between 0.6 to 0.8.

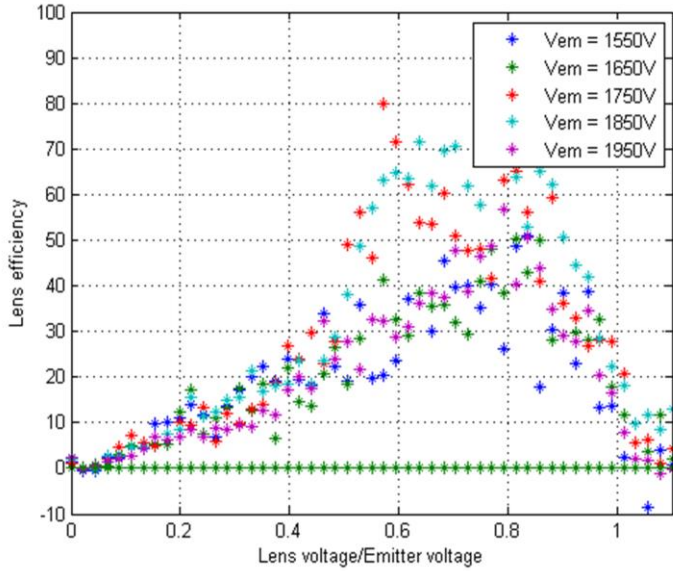


Figure 12. Measured lens efficiency of electrochemically etched and roughened tungsten needles for different emission voltages

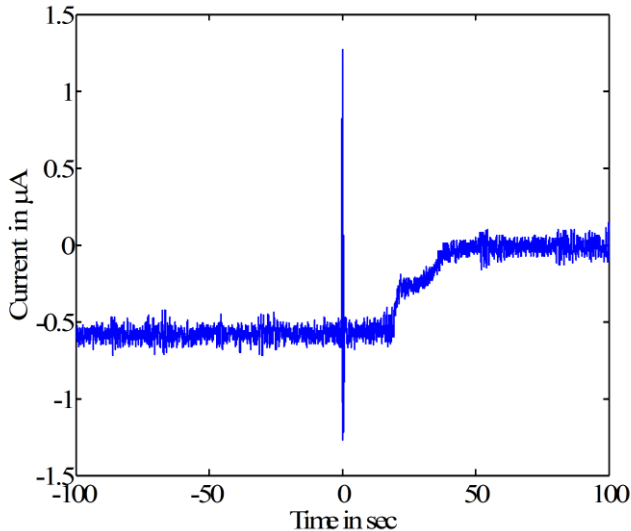


Figure 13. *ToF* trace from microfabricated capillary emitter in negative polarity of emission at $V_{em} = -1040$ V, $V_{lens} = -710$ V

needle emitters, this spread seems to be associated with the emission property of the capillary emitter itself which is not visible in case of the needle emitters. Retarded potential analysis of the spray energy spread of the capillary emitters may be useful in understanding this issue.

For the needle emitters, the efficiency can reach much higher values due to lower emission angle. Theoretically the system should be able to collect 100% of the emitted charges from the needles due to $15\text{--}20^\circ$ emission half-angle. Therefore, tests with the needles will be very helpful in characterizing the characteristics of the *ToF* system.

B. *ToF* measurement

ToF measurements have been performed on the capillary emitter by shutting the gate voltage from a value equal to $1.1 \times V_{em}$ to 0 V at a reference time and measuring the *ToF* from the traces of the detected current from the oscilloscope. In Fig. 13, the *ToF* trace of the capillary emitter is shown at $V_{em} = -1040$ V and $V_{lens} = -710$ V. The *ToF* of the BF_4^- ion obtained from the trace is $19.8 \mu\text{s}$. This is 1.46 times higher than the flight time of the BF_4^- ions at -1040 V emission voltage without the effect of the lens. Since V_{lens}/V_{em} ratio is 0.68, the *ToF correction factor* from simulation is 1.45 which is very close to the experimental value.

V. Conclusions

This paper reports the development of a *ToF* measurement system with an electrostatic ion-guide to increase the detected current. The ion-guide can focus a significant proportion of the charges emitted over a wide emission angle and with wide energy spread on a small detector at the end of a long flight tube. For micro-fabricated capillary emitters, the system can detect up to 40% of the charges emitted over 40° emission half-angle. This would help collecting the q/m information from a significant portion of the emitted beam rather than the portion that is mostly along the axis of the flight tube. The ion-guide has an effect of increased flight time of the charges and the effect can be modeled to a very good precision with the experimental value. The q/m can be mapped back from the delayed flight time by knowing the *ToF correction factor*.

For capillary emitters, the wide-spread range of V_{lens} for maximum efficiency and the peak between 200 V and 300 V are still not very clear. However, when compared with the

Acknowledgments

This work has been partially supported by the Swiss National Science Foundation 200021_146365, and by MicroThrust project, grant agreement number 263035, funded by the EC Seventh Framework Programme theme FP7-SPACE-2010.

References

¹Cotter R. J., *Time-of-flight Mass Spectrometry: Instrumentation and Applications in Biological Research*, 1st ed., ACS Professional Reference Books, Washington DC.

²Ataman C., Dandavino S. and Shea H., “Wafer-level integrated electrospray emitters for a pumpless microthruster system operating on high efficiency ion-mode” MEMS, Paris, France, 2012, pp. 1293–1296.

³Lozano P., Martínez-Sánchez M., “Ionic liquid ion sources: characterization of externally wetted emitters”, *Journal of Colloid and Interface Science* 282, 2005, pp. 415–421.

⁴Kroupn R., “Micromachined Electrospray Thrusters for Spacecraft Propulsion”, PhD Dissertation EDMI, EPFL, Switzerland, 2009.

⁵Chakraborty S., Ataman C., Dandavino S. and Shea H., “Microfabrication of an electrospray thruster for small spacecraft”, POWERMEMS, Atlanta, USA, 2012, p-073.

⁶Sise O., Ulu M. and Dogan M., “Multi-element cylindrical electrostatic lens systems for focusing and controlling charged particles”, *Nuclear Instruments and Methods in Physics Research Section A: Accelerators, Spectrometers, Detectors and Associated Equipment*, Vol. 554, Issues 1–3, 1 December 2005, pp. 114–131.

⁷<http://www.kimballphysics.com/ev-parts/stainless-steel-cylinders>.

⁸Dandavino S., Ataman C., Chakraborty S. and Shea H., “Design and fabrication of the thruster heads for the MicroThrust MEMS electrospray propulsion system”, IEPC 13, Washington DC, USA, 2013.